One-dimensional Anderson localization in certain correlated random potentials

P. Lugan, A. Aspect, and L. Sanchez-Palencia

Laboratoire Charles Fabry de l'Institut d'Optique, CNRS and Univ. Paris-Sud, Campus Polytechnique, RD 128,
F-91127 Palaiseau Cedex, France

D. Delande

Laboratoire Kastler-Brossel, UPMC, ENS, CNRS, 4 Place Jussieu, F-75005 Paris, France

B. Grémaud

Laboratoire Kastler-Brossel, UPMC, ENS, CNRS, 4 Place Jussieu, F-75005 Paris, France
and Centre for Quantum Technologies, National University of Singapore, 3 Science Drive 2, Singapore 117543, Singapore

C. A. Müller

Laboratoire Kastler-Brossel, UPMC, ENS, CNRS, 4 Place Jussieu, F-75005 Paris, France
and Physikalisches Institut, Universität Bayreuth, D-95440 Bayreuth, Germany

C. Miniatura

Centre for Quantum Technologies, National University of Singapore, 3 Science Drive 2, Singapore 117543, Singapore
and Institut Non Linéaire de Nice, UNS, CNRS, 1361 Route des Lucioles, F-06560 Valbonne, France

We study Anderson localization of ultracold atoms in weak one-dimensional speckle potentials using perturbation theory beyond Born approximation. We show the existence of a series of sharp crossovers (effective mobility edges) between energy regions where localization lengths differ by orders of magnitude. We also point out that the correction to the Born term explicitly depends on the sign of the potential. Our results are in agreement with numerical calculations in a regime relevant for experiments. Finally, we analyze our findings in the light of a diagrammatic approach.

I. INTRODUCTION

Anderson localization (AL) of single electron wave functions [1], first proposed to understand certain metal-insulator transitions, is now considered an ubiquitous phenomenon, which can happen for any kind of waves propagating in a medium with random impurities [2,3]. It can be understood as a coherent interference effect of waves multiply scattered from random defects, yielding localized waves with exponential profile and resulting in complete suppression of the usual diffusive transport associated with incoherent wave scattering [4]. So far, AL has been reported for light waves in diffusive media [5,6] and photonic crystals [7,8], sound waves [9], or microwaves [10]. Ultracold atoms have allowed studies of AL in momentum space [11,12] and recently direct observation of localized atomic matter waves [13,14].

In one-dimensional (1D) systems, all states are localized, and the localization length is simply proportional to the transport mean-free path [15]. However, this strong property should not hide that long-range correlations can induce subtle effects in 1D models of disorder, in particular those whose power spectrum has a finite support [16,17]. Examples are random potentials resulting from laser speckle and used in experiments with ultracold atoms [13,18,19]. Indeed, by construction [20], speckles have no Fourier component beyond a certain value $2k_c$, and the Born approximation predicts no backscattering and no localization for atoms with momentum $\hbar k > \hbar k_c$. This defines an *effective mobility edge* at $k = k_c$ [17], clear evidence of which has been reported [13].

Beyond this analysis—relevant for systems of moderate size [13,17]—study of AL in correlated potentials beyond the effective mobility edge requires more elaborated approaches. In Ref. [21], disorder with symmetric probability distribution was studied, and examples were exhibited, for which exponential localization occurs even for $k > k_c$ although with a much longer localization length than for $k < k_c$. It was also concluded that for Gaussian disorder, there is a second effective mobility edge at $2k_c$, while for non-Gaussian disorder, it is generally not so. These results do not apply to speckle potentials whose probability distribution is *asymmetric*. Moreover, although speckle potentials are not Gaussian, they derive from the squared modulus of a Gaussian field, and as we will show, the conclusions of Ref. [21] must be re-examined. Hence, considering speckle potentials presents a twofold interest. First, they form an original class of non-Gaussian disorder which can inherit properties of an underlying Gaussian process. Second, they are easily implemented in experiments with ultracold atoms where the localization length can be directly measured [13].

In this work, we study AL in speckle potentials beyond the Born approximation using perturbation theory [22], numerical calculations, and diagrammatic methods. We find that there exist several effective mobility edges at $k_c^{(p)} = pk_c$ with integer p, such that AL in the successive intervals $k_c^{(p-1)} < k < k_c^{(p)}$ results from scattering processes of increasing order. Effective mobility edges are thus characterized by sharp crossovers in the k dependence of the Lyapunov exponent (see Fig. 1). We prove this for the first two effective mobility edges by calculating the three lowest-order terms
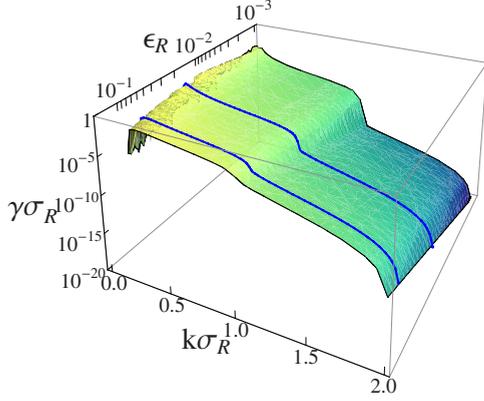
FIG. 1. (Color online) Lyapunov exponent γ calculated two orders beyond the Born approximation for particles in 1D speckle potentials created with a square diffusive plate versus the particle momentum $\hbar k$ and the strength of disorder $\epsilon_R = 2m\sigma_R^2 V_R/\hbar^2$ (V_R and σ_R are the amplitude and correlation length of the disorder). The solid blue lines correspond to $\epsilon_R = 0.1$ and $\epsilon_R = 0.02$.

and give general arguments for any p. In addition, we discuss the effect of odd terms that appear in the Born series due to the asymmetric probability distribution of speckle potentials.

II. SPECKLE POTENTIALS

Let us first recall the main properties of speckle potentials. Optical speckle is obtained by transmission of a laser beam through a medium with a random phase profile, such as a ground glass plate [20]. The resulting complex electric field $\mathcal{E}$ is a sum of independent random variables and forms a Gaussian process. In such a light field, atoms experience a random potential proportional to the intensity $|\mathcal{E}|^2$. Defining the zero of energies so that $\langle V \rangle = 0$, the random potential is thus

$$V(z) = V_R[|a(z/\sigma_R)|^2 - \langle |a(z/\sigma_R)|^2 \rangle], \qquad (1)$$

where the quantities $a(u)$ are complex Gaussian variables proportional to the electric field $\mathcal{E}$ and σ_R and V_R feature characteristic length and strength scales of the random potential (the precise definition of V_R and σ_R may depend on the model of disorder; see below). In contrast, $V(z)$ is not a Gaussian variable and its probability distribution is a decaying exponential, i.e., asymmetric. The sign of V_R is thus relevant and can be either positive or negative for "blue"- and "red"-detuned laser light, respectively. However, the random potential $V(z)$ inherits properties of the underlying Gaussian field $a(u)$. For instance, all potential correlators c_n are completely determined by the field correlator $c_a(u) = \langle a(0)^* a(u) \rangle$ via

$$\langle a_1^* \cdots a_p^* a_1 \cdots a_p \rangle = \sum_\Pi \langle a_1^* a_{\Pi(1)} \rangle \cdots \langle a_p^* a_{\Pi(p)} \rangle, \qquad (2)$$

where $a_{p'} = a(z_{p'}/\sigma_R)$ and Π describes the $p!$ permutations of $\{1, \ldots, p\}$. Hence, $c_2(u) = |c_a(u)|^2$ and defining $a(u)$ so that $\langle |a(u)|^2 \rangle = 1$, we have $\sqrt{\langle V(z)^2 \rangle} = |V_R|$. Also, since speckle results from interference between light waves of wavelength λ_L coming from a finite-size aperture of angular width 2α,

the Fourier transform of the field correlator has no component beyond $k_c = 2\pi \sin \alpha/\lambda_L$, and c_a has always a finite support:

$$\hat{c}_a(q) = 0 \quad \text{for } |q| > k_c\sigma_R \equiv 1. \qquad (3)$$

As a consequence, the Fourier transform of the potential correlator also has a finite support: $\hat{c}_2(q) = 0$ for $|q| > 2$.

III. PHASE FORMALISM

Consider now a particle of energy E in a 1D random potential $V(z)$ with zero statistical average [$V(z)$ need not be a speckle potential here]. The particle wave function ϕ can be written in phase-amplitude representation

$$\phi(z) = r(z)\sin[\theta(z)]; \quad \partial_z \phi = kr(z)\cos[\theta(z)], \qquad (4)$$

which proves convenient to capture the asymptotic decay of the wave function (here $k = \sqrt{2mE}/\hbar^2$ is the particle wave vector in the absence of disorder). It is easily checked that the Schrödinger equation is then equivalent to the coupled equations

$$\partial_z \theta(z) = k\{1 - [V(z)/E]\sin^2[\theta(z)]\}, \qquad (5)$$

$$\ln[r(z)/r(0)] = k\int_0^z dz'[V(z')/2E]\sin[2\theta(z')]. \qquad (6)$$

Since Eq. (5) is a closed equation for the phase θ, it is straightforward to develop the perturbation series of θ in increasing powers of V. Reintroducing the solutions at different orders into Eq. (6) yields the corresponding series for the amplitude $r(z)$ and the Lyapunov exponent:

$$\gamma(k) = \lim_{|z| \to \infty} \frac{\langle \ln[r(z)] \rangle}{|z|} = \sum_{n \geq 2} \gamma^{(n)}(k). \qquad (7)$$

The nth-order term $\gamma^{(n)}$ is thus expressed as a function of the n-point correlator $C_n(z_1, \ldots, z_{n-1}) = \langle V(0)V(z_1) \cdots V(z_{n-1}) \rangle$ of the random potential, which we write $C_n(z_1, \ldots, z_{n-1}) = V_R^n c_n(z_1/\sigma_R, \ldots, z_{n-1}/\sigma_R)$. Up order $n = 4$, we find

$$\gamma^{(n)} = \sigma_R^{-1}\left(\frac{\epsilon_R}{k\sigma_R}\right)^n f_n(k\sigma_R), \qquad (8)$$

where $\epsilon_R = 2m\sigma_R^2 V_R/\hbar^2$ and

$$f_2(\kappa) = +\frac{1}{4}\int_{-\infty}^0 du\, c_2(u)\cos(2\kappa u), \qquad (9)$$

$$f_3(\kappa) = -\frac{1}{4}\int_{-\infty}^0 du \int_{-\infty}^u dv\, c_3(u,v)\sin(2\kappa v), \qquad (10)$$

$$f_4(\kappa) = -\frac{1}{8}\int_{-\infty}^0 du \int_{-\infty}^u dv \int_{-\infty}^v dw\, c_4(u,v,w)\{2\cos(2\kappa w)$$
$$+ \cos[2\kappa(v+w-u)]\}. \qquad (11)$$

Note that the compact form (11) is valid provided that oscillating terms, which may appear from terms in c_4 that can be factorized as c_2 correlators, are appropriately regularized at
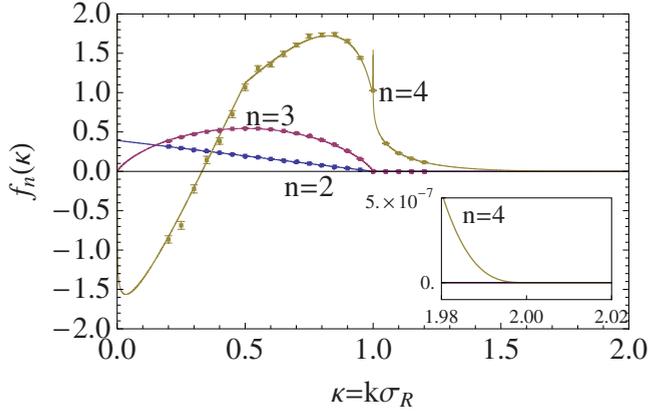
FIG. 2. (Color online) Functions f_n for $n=2$, 3, and 4 for a speckle potential created with a square diffusive plate [solid lines; see Eqs. (12) and (13) and the Appendix] and comparison with numerical calculations (points with error bars). The inset is a magnification of function f_4 around $\kappa=2$.
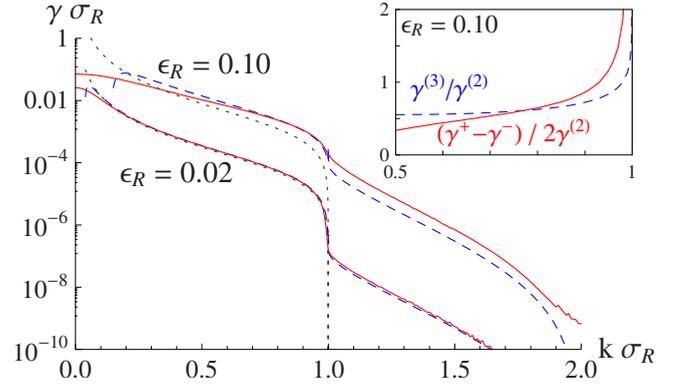

FIG. 3. (Color online) Lyapunov exponent $\gamma(k)$ versus the particle momentum k as determined numerically (solid red lines) and by perturbation theory up to order 4 (dashed blue lines) for a speckle potential created with a square plate. The dotted green lines are the Born term. Inset: comparison of odd and even contributions in the Born series for $\epsilon_R=0.1$.

infinity. Note also that in Eq. (8), the coefficients $(\epsilon_R/k\sigma_R)^n$ diverge for $k \to 0$, while the exact $\gamma(k)$ remains finite for any ϵ_R [23]. This signals a well-known breakdown of the perturbative approach. Conversely, the perturbative expansion is valid when $\gamma(k) \ll k$ (for $k \to 0$), i.e., when the localization length exceeds the particle wavelength, a physically satisfactory criterion.

IV. ONE-DIMENSIONAL ANDERSON LOCALIZATION IN SPECKLE POTENTIALS

A. Analytic results

Let us now examine the consequences of the peculiar properties of speckle potentials in the light of the above perturbative approach. For clarity, we restrict ourselves to 1D speckle potentials created by square diffusive plates as in Refs. [13,18] for which $c_a(u)=\sin(u)/u$ and $\hat{c}_a(q) \propto \Theta(1-|q|)$, where Θ is the Heaviside step function [24]. Using Eqs. (9) and (10), we find

$$f_2(\kappa) = \frac{\pi}{8}\Theta(1-\kappa)(1-\kappa), \quad (12)$$

$$f_3(\kappa) = -\frac{\pi}{4}\Theta(1-\kappa)[(1-\kappa)\ln(1-\kappa) + \kappa \ln(\kappa)]. \quad (13)$$

The functions f_2 and f_3 are simple and vanish for $\kappa \geq 1$ (see Fig. 2). This property is responsible for the existence of the first effective mobility edge at $k=k_c$ [17], such that $\gamma(k)\sigma_R \sim (\epsilon_R/k\sigma_R)^2$ for $k \lesssim \sigma_R^{-1}$ while $\gamma(k)\sigma_R = O(\epsilon_R/k\sigma_R)^4$ for $k \gtrsim \sigma_R^{-1}$. The fact that f_3 vanishes in the same interval ($\kappa \geq 1$) as f_2 exemplifies the general property that odd-n terms cannot be leading terms in any range of k because $\gamma(k)$ must be positive whatever the sign of V_R. For $\kappa < 1$ however, $f_3(\kappa)$ is not identically zero owing to the asymmetric probability distribution in speckle potentials. The term $\gamma^{(3)}$ can thus be either positive or negative depending on the sign of V_R [22].

The function f_4 is found similarly from Eq. (11). While its expression is quite complicated (see the Appendix), its be-

havior is clear when plotted (see Fig. 2). Let us emphasize some of its important features. First, there is a discontinuity of the derivative of f_4 at $\kappa=1/2$. Second, we find a very narrow logarithmic divergence, $f_4(\kappa) \sim -(\pi/32)\ln|1-\kappa|$ at $\kappa=1$, which signals a singularity of the perturbative approach (note that it does not appear in Fig. 1 due to finite resolution of the plot). Finally, the value $\kappa=2$ corresponds to the boundary of the support of f_4, showing explicitly the existence of a second effective mobility edge at $k=2\sigma_R^{-1}$. Hence, while $\gamma(k)\sigma_R \sim (\epsilon_R/k\sigma_R)^4$ for $k \lesssim 2\sigma_R^{-1}$, we have $\gamma(k)\sigma_R = O(\epsilon_R/k\sigma_R)^6$ for $k \gtrsim 2\sigma_R^{-1}$, since $f_4(\kappa)$ as well as $f_5(\kappa)$ vanish for $\kappa \geq 2$.

B. Numerics

In order to test the validity of the perturbative approach for experimentally relevant parameters, we have performed numerical calculations using a transfer matrix approach. The results are plotted in Fig. 3: $\epsilon_R=0.02$ corresponds to $V_R/\hbar = 2\pi \times 16$ Hz in Fig. 3 of Ref. [13] and $\epsilon_R=0.1$ to $V_R/\hbar = 2\pi \times 80$ Hz in Fig. 3 and to Fig. 4 of Ref. [13]. For $\epsilon_R = 0.02$, the agreement between analytical and numerical results is excellent. The effective mobility edge at $k=\sigma_R^{-1}$ is very clear: we find a sharp step for $\gamma(k)$ of about 2 orders of magnitude. For $\epsilon_R=0.1$, we find the same trend but with a smoother and smaller step (about one order of magnitude). In this case, although the Born term for $k \lesssim \sigma_R^{-1}$ and the fourth-order term for $k \gtrsim \sigma_R^{-1}$ provide reasonable estimates (within a factor of 2), higher-order terms—which may depend on the sign of V_R—contribute significantly.

The contribution of the odd terms can be extracted by taking $\gamma^+ - \gamma^-$, where $\gamma^\pm$ are the Lyapunov exponents obtained for positive and negative disorder amplitude of same modulus $|V_R|$, respectively. As shown in the inset of Fig. 3, the odd terms range from 30% to 70% of the Born term for $0.6 \lesssim k\sigma_R \lesssim 0.9$ and $\epsilon_R=0.1$ and are of the order of $\gamma^{(3)}$ in weak disorder and away from the divergence at $k=\sigma_R^{-1}$. This shows that the first correction $\gamma^{(3)}$ to the Born term can be relevant in experiments.

For completeness, we have calculated the $f_n(\kappa)$ as the coefficients of fits in powers of $\epsilon_R/k\sigma_R$ using series of calculations of $\gamma(k)$ at fixed k and various ϵ_R. As shown in Fig. 2, the agreement with the analytic formulas is excellent. In particular, the numerics reproduce the predicted kink at $\kappa = 1/2$. The logarithmic singularity around $\kappa = 1$ being very narrow, we did not attempt to study it.

V. DIAGRAMMATIC ANALYSIS

Let us finally complete our analysis using diagrammatic methods, which allow us to exhibit momentum exchange in scattering processes as compact graphics and thus to identify effective mobility edges in a quite general way. In 1D, the localization length can be calculated from the backscattering probability of $\langle |\psi|^2 \rangle$ using quantum transport theory. The irreducible diagrams of elementary scattering processes in speckle potentials have been identified in Ref. [25].

To lowest order in ϵ_R (Born approximation), the average intensity of a plane wave with wave vector k backscattered by the random potential is described by

$$U_2(k) = q + k \begin{matrix} k \to \bullet \leftarrow k \\ \swarrow \quad \searrow \\ k \leftarrow \bullet \to k \end{matrix} q - k =: \begin{matrix} k \to \otimes \leftarrow k \\ \downarrow 2k \\ k \leftarrow \otimes \to k \end{matrix} .$$

$$(14)$$

The upper part of the diagram represents ψ (particle) and the lower part its conjugate ψ^* (hole). The dotted line $\bullet \cdots \overset{q}{\cdots} \cdots \bullet = \epsilon_R \hat{c}_a(q)$ represents the field correlator; simple closed loops over field correlations can be written as a potential correlation $\otimes \cdots \cdots \cdots \otimes$. Backscattering requires diagram (14) to channel a momentum $2k$, entering at the particle, down along the potential correlations to the hole. Therefore, the diagram vanishes for $k\sigma_R > 1$.

At order ϵ_R^3, the only possible contribution is

$$U_3(k) = q + k \begin{matrix} & \overset{\nearrow\cdots\nwarrow}{} & \\ k \to & \bullet\!\!\longrightarrow\!\!\bullet & \leftarrow k \\ & \overset{p}{} & \\ \searrow & & \swarrow \\ k \leftarrow & \bullet & \to k \end{matrix} q - k + \text{c.c.}$$

$$(15)$$

The straight black line stands for the particle propagator $[E_k - E_p + i0]^{-1}$ at intermediate momentum p. Diagram (15) features two vertical field correlation lines, just as diagram (14), and thus vanishes at the same threshold $k = \sigma_R^{-1}$. Evaluating two-loop diagram (15), we recover precisely contribution (13).

Many diagrams contribute to order ϵ_R^4. First there are the usual backscattering contributions with pure intensity correlations [Figs. 4(a)–4(c)]. Both Figs. 4(a) and 4(c) have a single vertical intensity correlation and vanish for $k > \sigma_R^{-1}$. In contrast, the crossed diagram [Fig. 4(b)] has two vertical intensity correlation lines and can thus accommodate momenta up to $k = 2\sigma_R^{-1}$. Performing the integration, we find that this diagram reproduces those contributions to $f_4(\kappa)$ for $\kappa \in [1,2]$ that contain factorized correlators (see the Appendix). Second, there are nine more diagrams, all with nonfactorizable field correlations [25]. A single one has not two, but
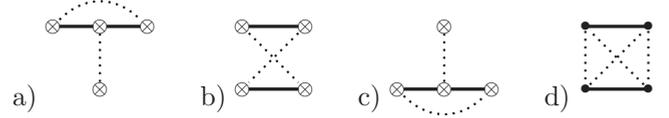

FIG. 4. Relevant fourth-order backscattering contributions. Contrary to the case of uncorrelated potentials [26,27], the sum of diagrams (a)–(c) *does not* give zero for speckle potentials; only diagrams (b) and (d) contribute for $k\sigma_R \in [1,2]$.

four vertical field correlation lines, shown in Fig. 4(d), and contributes for $k\sigma_R \in [1,2]$. Carrying out the three-loop integration, we recover exactly the nonfactorizable contributions to $f_4(\kappa)$ for $\kappa \in [1,2]$.

VI. CONCLUSION

We have developed perturbative and diagrammatic approaches beyond the Born approximation, suitable to study 1D AL in correlated disorder with possibly asymmetric probability distribution. In speckle potentials, the k dependence of the Lyapunov exponent exhibits sharp crossovers (effective mobility edges) separating regions where AL is due to scattering processes of increasing order. We have shown it explicitly for $k = \sigma_R^{-1}$ and $k = 2\sigma_R^{-1}$, and we infer that there is a series of effective mobility edges at $k = p\sigma_R^{-1}$ with integer p since, generically, diagrams with $2p$ field correlations or p intensity correlations can contribute up to $k = p\sigma_R^{-1}$. This is because, although speckles are not Gaussian, they derive from a Gaussian field. Finally, exact numerics support our analysis for experimentally relevant parameters and indicate the necessity to use higher-order terms in the Born series even for $k < \sigma_R^{-1}$. Hence, important features that we have pointed out, such as odd terms in the Born series for $k < \sigma_R^{-1}$ and exponential localization for $k > \sigma_R^{-1}$, should be observable experimentally.

APPENDIX

Here, we give the explicit formula of the function $f_4(\kappa)$ for a speckle potential created by a square diffusive plate, such that the fourth-order term in the Born expansion of the Lyapunov exponent γ reads

$$\gamma^{(4)} = \sigma_R^{-1}\left(\frac{\epsilon_R}{k\sigma_R}\right)^4 f_4(k\sigma_R).$$

The function $f_4(\kappa)$ is the sum of three terms with different supports:

$$f_4(\kappa) = f_4^{[0,1/2]}(\kappa) + f_4^{[0,1]}(\kappa) + f_4^{[1,2]}(\kappa),$$

where $f_4^{[\alpha,\beta]}(\kappa)$ lives on the interval $\kappa \in [\alpha, \beta]$ and

$$f_4^{[0,1/2]}(\kappa) = -\frac{\pi^3}{16}(1 - 2\kappa),$$

$$
\begin{aligned}
f_4^{[0,1]}(\kappa) = \frac{\pi}{16}\Bigg\{ &4 - 6\kappa - \frac{10\pi^2}{3}(1 - 2\kappa) - (4 - 2\kappa)\ln(\kappa) - \left(\frac{5}{\kappa} - 3\kappa\right)\ln(1 - \kappa) + \left(\frac{1}{\kappa} + \kappa\right)\ln(1 + \kappa) - (4 - 8\kappa)\ln^2(\kappa) \\
&+ 22(1 - \kappa)\ln^2(1 - \kappa) + (18 + 14\kappa)\ln^2(1 + \kappa) - 16(1 - \kappa)\ln(1 - \kappa)\ln(\kappa) - 4(1 - \kappa)\ln(1 - \kappa)\ln(1 + \kappa) \\
&- 32(1 + \kappa)\ln(\kappa)\ln(1 + \kappa) - 24(1 + \kappa)\mathrm{Li}_2(\kappa) + 32(1 + \kappa)\mathrm{Li}_2\left(\frac{\kappa}{1 + \kappa}\right) - 8\kappa\mathrm{Li}_2\left(\frac{2\kappa}{1 + \kappa}\right) - 8(1 - 2\kappa)\mathrm{Li}_2\left(2 - \frac{1}{\kappa}\right)\Bigg\},
\end{aligned}
$$

$$
f_4^{[1,2]}(\kappa) = \frac{\pi}{32}\Bigg\{ -2 + \left(1 + \frac{\pi^2}{3}\right)\kappa + 4\kappa\mathrm{Li}_2(1 - \kappa) - \left(\frac{2}{\kappa} - 2 + \kappa\right)\ln(\kappa - 1) - 2(\kappa - 1) - \ln^2(\kappa - 1) + 4\kappa\ln(\kappa - 1)\ln(\kappa)\Bigg\},
$$

where $\mathrm{Li}_2(z) = \int_z^0 dt\, \ln(1 - t)/t = \Sigma_{k=1}^{\infty} z^k/k^2$ is the dilogarithm function.

---

[1] P. W. Anderson, Phys. Rev. **109**, 1492 (1958).
[2] E. Akkermans and G. Montambaux, *Mesoscopic Physics of Electrons and Photons* (Cambridge University Press, New York, 2006).
[3] B. van Tiggelen, in *Wave Diffusion in Complex Media*, edited by J. P. Fouque, Lecture Notes at Les Houches 1998, NATO Science (Kluwer, Dordrecht, 1999).
[4] P. A. Lee and T. V. Ramakrishnan, Rev. Mod. Phys. **57**, 287 (1985).
[5] D. S. Wiersma, P. Bartolini, A. Lagendijk, and R. Righini, Nature (London) **390**, 671 (1997).
[6] M. Störzer, P. Gross, C. M. Aegerter, and G. Maret, Phys. Rev. Lett. **96**, 063904 (2006).
[7] T. Schwartz, G. Bartal, S. Fishman, and M. Segev, Nature (London) **446**, 52 (2007).
[8] Y. Lahini, A. Avidan, F. Pozzi, M. Sorel, R. Morandotti, D. N. Christodoulides, and Y. Silberberg, Phys. Rev. Lett. **100**, 013906 (2008).
[9] H. Hu, A. Strybulevytch, J. H. Page, S. E. Skipetrov, and B. A. van Tiggelen, Nat. Phys. **4**, 945 (2008).
[10] A. A. Chabanov, M. Stoytchev, and A. Z. Genack, Nature (London) **404**, 850 (2000).
[11] F. L. Moore, J. C. Robinson, C. F. Bharucha, B. Sundaram, and M. G. Raizen, Phys. Rev. Lett. **75**, 4598 (1995).
[12] J. Chabé, G. Lemarié, B. Grémaud, D. Delande, P. Szriftgiser, and J. C. Garreau, Phys. Rev. Lett. **101**, 255702 (2008).
[13] J. Billy, V. Josse, Z. Zuo, A. Bernard, B. Hambrecht, P. Lugan, D. Clément, L. Sanchez-Palencia, P. Bouyer, and A. Aspect, Nature (London) **453**, 891 (2008).

[14] G. Roati, C. D'Errico, L. Fallani, M. Fattori, C. Fort, M. Zaccanti, G. Modugno, M. Modugno, and M. Inguscio, Nature (London) **453**, 895 (2008).
[15] C. W. J. Beenakker, Rev. Mod. Phys. **69**, 731 (1997).
[16] F. M. Izrailev and A. A. Krokhin, Phys. Rev. Lett. **82**, 4062 (1999).
[17] L. Sanchez-Palencia, D. Clément, P. Lugan, P. Bouyer, G. V. Shlyapnikov, and A. Aspect, Phys. Rev. Lett. **98**, 210401 (2007); L. Sanchez-Palencia, D. Clément, P. Lugan, P. Bouyer, and A. Aspect, New J. Phys. **10**, 045019 (2008).
[18] D. Clément, A. F. Varón, J. A. Retter, L. Sanchez-Palencia, A. Aspect, and P. Bouyer, New J. Phys. **8**, 165 (2006).
[19] L. Fallani, C. Fort, and M. Inguscio, Adv. At., Mol., Opt. Phys. **56**, 119 (2008).
[20] J. W. Goodman, *Speckle Phenomena in Optics: Theory and Applications* (Roberts and Co., Englewood, 2007).
[21] L. Tessieri, J. Phys. A **35**, 9585 (2002).
[22] See also E. Gurevich and O. Kenneth, Phys. Rev. A **79**, 063617 (2009).
[23] B. Derrida and E. Gardner, J. Phys. **45**, 1283 (1984).
[24] Our results can be extended to any 1D random potential that fulfill conditions (1)–(3) with similar conclusions.
[25] R. C. Kuhn, C. Miniatura, D. Delande, O. Sigwarth, and C. A. Müller, New J. Phys. **9**, 161 (2007).
[26] I. V. Gornyi, A. D. Mirlin, and D. G. Polyakov, Phys. Rev. B **75**, 085421 (2007).
[27] A. Cassam-Chenai, and B. Shapiro, J. Phys. I (France) **4**, 1527 (1994).